Acta Crystallographica Section D
**Biological Crystallography**
ISSN 0907-4449

# Slow diffusion of lactose out of galectin-3 crystals monitored by X-ray crystallography: possible implications for ligand-exchange protocols

**Patrick M. Collins,[a] Kazuya I. P. J. Hidari[b] and Helen Blanchard[a]***

[a]The Institute for Glycomics, Griffith University (Gold Coast Campus), PMB 50 Gold Coast Mail Centre, Queensland 9726, Australia, and [b]Department of Biochemistry, University of Shizuoka, School of Pharmaceutical Sciences, 52-1 Yada, Suruga-ku, Shizuoka-shi, Shizuoka 422-8526, Japan

Correspondence e-mail: h.blanchard@griffith.edu.au

Received 25 October 2006
Accepted 5 December 2006

**PDB References:** human galectin-3 carbohydrate-recognition domain, 2nn8, r2nn8sf; 2nmo, r2nmosf; 2nmn, r2nmnsf.

Galectin-3 is a multifunctional carbohydrate-binding protein that has roles in cancer progression. In addition to carbohydrate-dependent extracellular functions, galectin-3 participates in carbohydrate-independent intracellular signalling pathways, including apoptosis, *via* protein–protein interactions, some of which engage the carbohydrate-binding groove. When ligands bind within this site, conformational rearrangements are induced and information on unliganded galectin-3 is therefore valuable for structure-based drug design. Removal of cocrystallized lactose from the human galectin-3 carbohydrate-recognition domain was achieved *via* crystal soaking, but took weeks despite low affinity. Pre-soaking to remove lactose enabled the subsequent binding of cryoprotectant glycerol, whereas when the lactose was not removed *a priori* the glycerol could not displace it in the short cryosoaking time frame. This slow diffusion of lactose out of the crystals contrasts with the entrance of glycerol, which takes place within minutes. The importance of the removal of incumbent ligands prior to attempts to introduce alternative ligands is indicated, even for proteins exhibiting low affinity for ligands, and has significance for ligand exchange in structure-based drug design.

## 1. Introduction

Protein X-ray crystallography is a powerful component of structure-aided drug design (SADD) and provides an atomic resolution structure of the target macromolecule, preferably in complex with a small-molecule ligand, thus providing information on protein–ligand interactions; it is indispensable for inhibitor design. Two major techniques for obtaining protein–ligand complexes are cocrystallization, which involves *ab initio* crystal growth of the protein–ligand complex, and crystal soaking, which involves diffusion of ligands into either pre-formed apo crystals or ligand exchange with previously cocrystallized ligands (Danley, 2006). Ligand exchange is used extensively in SADD and can be excellent for quickly determining the binding modes of synthetic inhibitors (McNae *et al.*, 2005). Proteins known to have weak ligand affinity, such as carbohydrate-recognition proteins, might be anticipated as easily permitting ligand substitution and without prior removal of the incumbent ligand. Some proteins only crystallize in the presence of ligand and, given that incoming and outgoing ligands are generally of similar affinity at the early drug-design stages, it is important to establish experimental approaches that most efficiently enable exchange with the new ligand.

The carbohydrate-binding protein galectin-3 has affinity for $\beta$-galactoside sugars (Barondes *et al.*, 1994) and, as with other lectins, binds carbohydrates with low affinity. For example, the $K_d$ of lactose for the galectin-3 carbohydrate-recognition domain (CRD) is 260 $\mu M$, as determined by frontal affinity chromatography (Hirabayashi *et al.*, 2002). Human galectin-3 is involved in intracellular and extracellular processes and many aspects of cancer progression, such as the promotion of angiogenesis (Ochieng *et al.*, 2004), cell–cell and cell–matrix adhesion (Hughes, 2001), the prevention of killing by T cells (Stillman *et al.*, 2006) and the prevention of apoptosis induced by chemotherapeutic drugs (Takenaka *et al.*, 2004). The intracellular protein form has tumour-promoting anti-apoptotic properties that are ascribed to protein–protein interactions, and since most intracellular proteins are not glycosylated, these interactions are expected

to be independent of carbohydrate binding. Interestingly however, these protein–protein interactions can occur within the carbohydrate-binding site, as exemplified by association with the Bcl-2 repressor of apoptosis *via* the NWGR anti-death motif that resides within this site in galectin-3 (Yang *et al.*, 1996). The crystallographic structure (2.1 Å) of human galectin-3 CRD with bound *N*-acetyllactosamine (LacNAc) comprises a $\beta$-sandwich fold with a shallow binding groove that interacts mainly with the galactose moiety of LacNAc (Seetharaman *et al.*, 1998). No X-ray crystal structure of apo galectin-3 is available, but NMR has indicated ligand-induced conformational changes of loops around the binding site (Umemoto *et al.*, 2003). This crystal form of galectin-3 is amenable to ligand-exchange soaking techniques, revealing rearrangement of some binding-site amino acids upon binding higher affinity synthetic inhibitors (Sorme *et al.*, 2005). By soaking (in reservoir solution) crystals of human galectin-3 CRD initially containing bound lactose, we have generated structures in which the carbohydrate ligand is gradually substituted, providing insight into the diffusion times associated with such low-affinity ligands, which are important for consideration in the ligand-exchange protocols associated with drug design.

## 2. Experimental

### 2.1. Cloning, expression and purification

Primers for polymerase chain reaction (PCR) were designed using the nucleotide sequence of human galectin-3 (GenBank accession No. M57710; Robertson *et al.*, 1990). The primer sequences used to amplify the entire coding region of human galectin-3 cDNA were a forward primer containing an *Nde*I site (5′-CATATGGCAGACAATTTTTCGCTC-3′) and a reverse primer containing a *Bam*HI site (5′-GGATCCTTATATCATGGTATATGAAGCAC-3′), corresponding to nucleotide positions 19–39 and 749–771 of human galectin-3, respectively. PCR was performed using Gene Pool Human Normal Liver cDNA as a template (Saiki *et al.*, 1985). The resultant 765 bp amplified DNA was cloned into pET-3a vector (Novagen, USA) and introduced into *Escherichia coli* strain JM109. Full-length galectin-3 protein expression was induced in log-phase culture [*E. coli* strain BL21 (DE3) containing pET-3a-Gal-3 vector] by the addition of 0.4 m*M* isopropyl $\beta$-D-thiogalactoside. After 3–4 h expression, cells were harvested and lysed using 2 mg ml$^{-1}$ lysozyme (Fluka) supplemented with 1%(*w*/*v*) Triton X-100 and 50 µg ml$^{-1}$ DNaseI (Roche Diagnostics). Galectin-3 was purified from cell-lysate supernatant by affinity chromatography using a lactosyl-Sepharose column (Levi & Teichberg, 1981) with elution buffer comprising 100 m*M* lactose in phosphate-buffered saline (PBS) pH 7.4 as described by Leffler *et al.* (1989). Isolation of the galectin-3 CRD fragment from purified full-length galectin-3 was achieved by incubation in buffer containing 2 m*M* $CaCl_2$ at 277 K for 1–2 d followed by centrifugation to remove insoluble material. This procedure differed from that reported previously, in which the CRD was obtained by performing a digestion *via* direct addition of type VII collagenase (Massa *et al.*, 1993), which removes the galectin-3 repetitive domain. Collagenase is copurified with galectin-3 and given that its activity is dependent on calcium ions (Gallop *et al.*, 1957), our protocol thus led to the generation of galectin-3 CRD (residues 108–250) without the requirement for recombinant collagenase.

### 2.2. Crystallization and crystal soaking

Crystallization of the galectin-3 CRD with bound lactose was achieved using methods similar to those reported previously (Seetharaman *et al.*, 1998). The protein was crystallized using the hanging-drop vapour-diffusion method with 4 µl drops consisting of equal volumes of protein solution (100 m*M* lactose in PBS pH 7.5 supplemented with 2 m*M* $CaCl_2$ and a protein concentration of 10 mg ml$^{-1}$) and reservoir solution [100 m*M* Tris–HCl pH 7.0, 31%(*w*/*v*) PEG 6000, 100 m*M* $MgCl_2$ and 8 m*M* $\beta$-mercaptoethanol]. Crystals formed within two weeks and attained typical dimensions of 0.1 × 0.1 × 0.5 mm. In order to soak lactose from the galectin-3-binding site, crystals were transferred from the hanging drops using a cryo-loop, placed briefly in 20 µl drops of reservoir solution and then placed in 1 ml volumes of reservoir solution for soaking. Soaking times and fresh solution changes were as follows: a 20 min soak (2 × 10 min in fresh solution), a 12 h soak (1 × 2 h, 1 × 8 h, 1 × 2 h), a 17 d soak (3 × 3 d, 2 × 4 d, 1 × 2 h) and a 29 d soak (2 × 3 d, 5 × 4 d, 1 × 3 d, 1 × 2 h).

### 2.3. Data collection, structure determination and refinement

X-ray diffraction data sets were collected at room temperature from galectin-3 CRD crystals mounted in 0.7 mm quartz capillaries on a ProteumR (Bruker AXS, Madison, WI, USA) diffractometer with a MacScience M06X$^{CE}$ rotating-anode generator equipped with a SMART6000 CCD detector. For cryotemperature synchrotron X-ray diffraction experiments, crystals were soaked (5–180 s) in drops containing reservoir solution supplemented with 15%(*v*/*v*) glycerol prior to mounting in nylon cryo-loops (Hampton Research) and flash-cooled in liquid nitrogen. Synchrotron X-ray diffraction data sets were collected at beamline 8.3.1 at the Advanced Light Source (100 K, $\lambda$ = 1.1159 Å) using an ADSC CCD detector. In-house X-ray diffraction data were integrated using *SAINT* and scaled and merged using *PROSCALE* (Bruker AXS, Madison, WI, USA). Synchrotron data were integrated using *MOSFLM* (Leslie, 2006) directly or automatically within *ELVES* (Holton & Alber, 2004) and scaled using *SCALA* (Evans, 1993) as implemented in the *CCP*4 suite of crystallographic software (Collaborative Computational Project, Number 4, 1994). Refinement was performed using *REFMAC*5 (Murshudov *et al.*, 1997) with the published human galectin-3 CRD

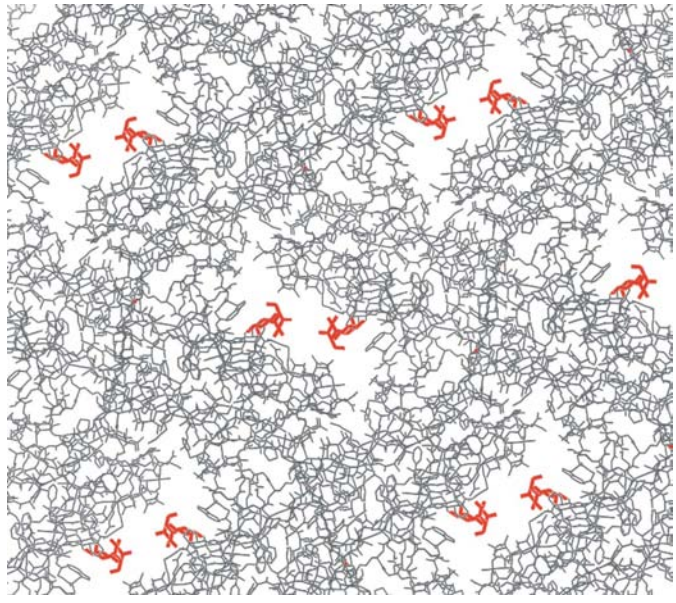

**Figure 1**
Crystal packing along unit-cell axis *a*, to which the solvent channels run parallel in human galectin-3 CRD crystals, with bound lactose (bold bonds) protruding into the channels.

structure (identical sequence consisting of residues 114–250) stripped of nonprotein atoms as the initial model (PDB code 1a3k; Seetharaman *et al.*, 1998). Visualization of electron density and model building was performed using either *O* (Jones *et al.*, 1991) and/or *Coot* (Emsley & Cowtan, 2004). Final structure validation was performed using *SFCHECK* (Collaborative Computational Project, Number 4, 1994) and *PROCHECK* (Laskowski *et al.*, 1993).

## 3. Results and discussion

Crystallization of galectin-3 CRD with bound lactose gave an orthorhombic crystal form, space group $P2_12_12_1$, with one galectin-3 CRD molecule per asymmetric unit. The refined structure from these galectin-3–lactose crystals is highly comparable to the previously reported LacNAc-bound galectin-3 CRD structures (PDB code 1a3k, Seetharaman *et al.*, 1998; PDB code 1kjl, Sorme *et al.*, 2005). No systematic differences are observed between the structures determined at room temperature and 100 K and the superimposition of these structures with each other and with our three structures gave r.m.s. deviations on $C^{\alpha}$ atoms in the range 0.071–0.232 Å. As with the previously reported structures, the initial residues at the N-terminus of the CRD fragment are not visible owing to disorder and Pro113 is the first residue for which electron density is interpretable. In all three structures reported here, Arg144 (within the binding site) is in the same conformation as in the previously reported LacNAc structure (PDB code 1kjl; Sorme *et al.*, 2005) as opposed to the alternate conformation induced by a 3′-derivative of LacNAc (PDB code 1kjr; Sorme *et al.*, 2005). A chloride ion is observed in our low-temperature structures at an identical site, distal to the carbohydrate-binding region, to the previously published galectin-3 CRD cryo-structures (Sorme *et al.*, 2005). This ion is not detected in the room-temperature structures that we report here or in that previously reported by Seetharaman *et al.* (1998). The major solvent channels in this crystal form run parallel to unit-cell axis *a* and have dimensions of ∼20 × 8 Å (Fig. 1). The carbohydrate-binding site is shallow, unobstructed and adjacent to the solvent channels and we anticipated that removal of the low-affinity lactose would be achieved rapidly.

Electron density clearly defines the lactose bound within the carbohydrate-binding site of the galectin-3 CRD (Fig. 2*a*; PDB code 2nn8; Table 1). The conformation of lactose in the binding site is identical to that in the previously reported LacNAc-bound structures (PDB code 1a3k, Seetharaman *et al.*, 1998; PDB code 1kjl, Sorme *et al.*, 2005) and the LacNAc moiety of the inhibitor-bound structure (PDB code 1kjr; Sorme *et al.*, 2005). In our structures, the electron density reveals that both the $\alpha$ and $\beta$ anomers of lactose (a reducing sugar) are bound to protein and with equal occupancy within the crystal. Consequently, we have refined the model with 50% occupancies for each of the anomeric O atom (O1) positions. A mixture of the two anomers of lactose is in accordance with the fact that they exist in equilibrium in aqueous solution, exhibiting a ratio of 37.3% $\alpha$ lactose and 62.7% $\beta$ lactose (Kendrew & Moelwyn-Hughes, 1940). After soaking galectin-3 lactose cocrystals in reservoir solution for 20 min and for 12 h, the electron density revealed that lactose was still bound and with estimated occupancies of greater than 90% and

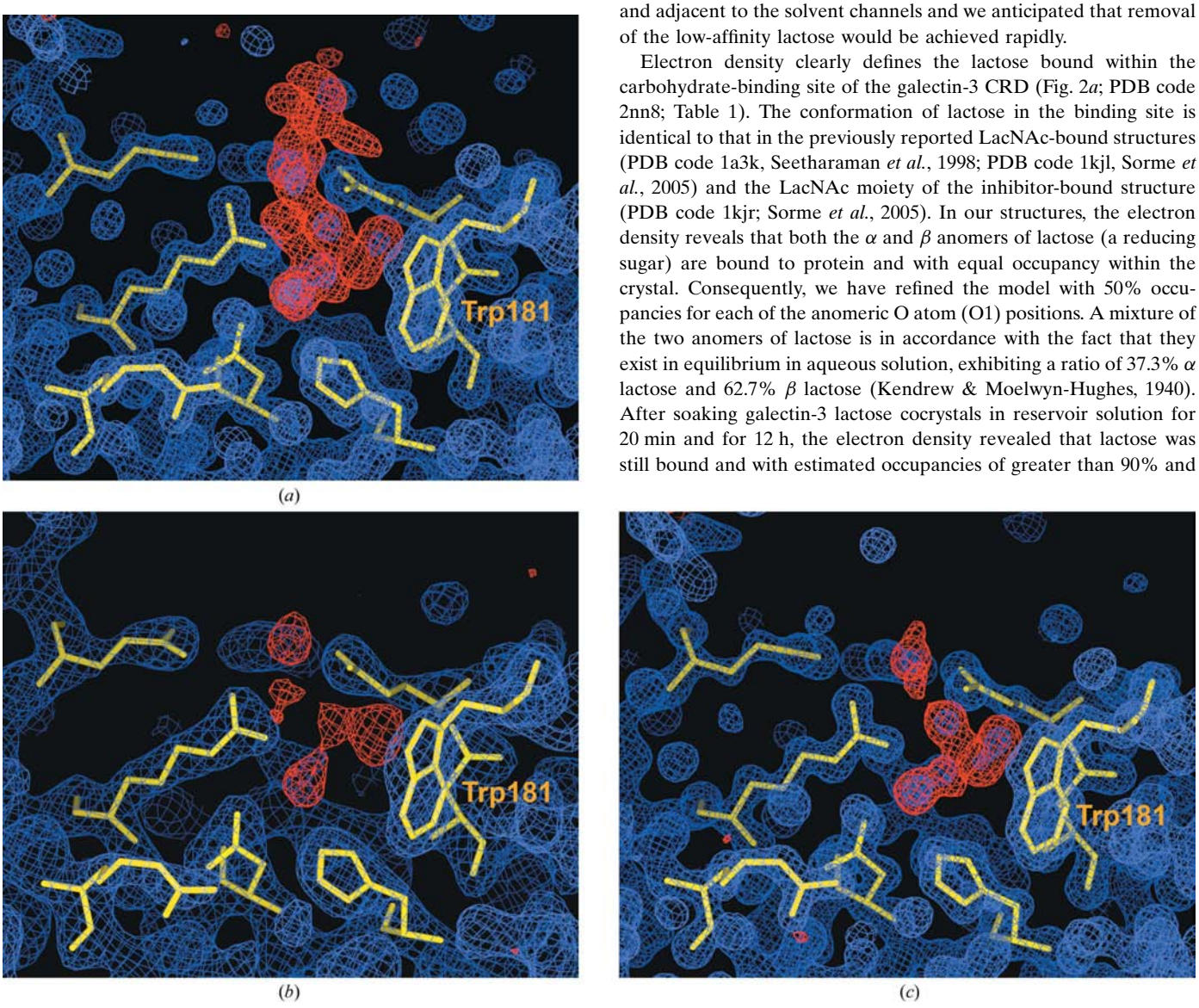


**Figure 2**
The binding site of human galectin-3 CRD for (*a*) a lactose-bound structure (1.35 Å), (*b*) a crystal soaked for 17 d in reservoir solution, revealing bound water molecules (2.45 Å), and (*c*) a crystal soaked for 29 d in reservoir solution, revealing glycerol in the binding site (1.35 Å). The figures show an identical region of the binding site. Electron density was calculated prior to addition of ligand to the model, with important amino-acid side chains shown as yellow bonds. The $2|F_o| - |F_c|$, $\alpha_c$ map contoured at $1.5\sigma$ is shown as blue density and the $|F_o| - |F_c|$, $\alpha_c$ map contoured at $3.5\sigma$ as red density.

**Table 1**
Data-collection and refinement statistics for galectin-3 CRD structures with bound lactose, glycerol and waters within the carbohydrate-binding site.

Atomic coordinates and structure factors associated with the 20 min and 12 h soak are available upon request. Values in parentheses are for the highest resolution shell.

| Contents of binding site | Lactose | Glycerol | Waters |
|---|---|---|---|
| PDB code | 2nn8 | 2nmo | 2nmn |
| Data collection | | | |
| Temperature (K) | 100 | 100 | 295 |
| Unit-cell parameters (Å) | $a$ = 36.4, $b$ = 57.8, $c$ = 62.6 | $a$ = 36.3, $b$ = 57.6, $c$ = 62.2 | $a$ = 37.3, $b$ = 58.2, $c$ = 63.7 |
| Resolution (Å) | 1.35 (1.42–1.35) | 1.35 (1.42–1.35) | 2.45 (2.56–2.45) |
| Total observations | 109139 | 105938 | 20233 |
| Unique reflections | 29182 | 28612 | 5400 |
| $R_{merge}$ (%) | 3.6 (21.3) | 3.8 (18.6) | 4.8 (18.7) |
| Completeness (%) | 98.3 (89.9) | 97.6 (87.3) | 98.4 (84.1) |
| $I/\sigma(I)$ | 11.5 (3.4) | 9.7 (4.9) | 11.4 (4.6) |
| Refinement | | | |
| Resolution range for refinement (Å) | 42–1.35 | 31–1.35 | 43–2.45 |
| No. of protein residues | 138 | 138 | 138 |
| No. of water molecules | 197 | 170 | 54 |
| R.m.s.d. bond lengths (Å) | 0.007 | 0.007 | 0.016 |
| R.m.s.d. bond angles (°) | 1.29 | 1.29 | 1.69 |
| $R$ factor (%) | 16.4 | 16.9 | 16.3 |
| $R_{free}$ (%) (based on 5% of data) | 17.5 | 18.4 | 23.7 |
| Overall Wilson $B$ factors (Å$^2$) | 12.1 | 11.2 | 44.2 |
| Average $B$ factors (Å$^2$) | | | |
| Protein atoms | 11.3 | 10.7 | 23.7 |
| Ligand atoms: nonlactose/lactose | —/19.0 | 11.8/14.2 | 24.4/29.0 |
| Water molecules | 28.6 | 27.8 | 27.0 |
| Soak time (crystal soaked in reservoir solution) (d) | 0 | 29 | 17 |
| Estimated occupancy of lactose (%) | 100 | 30 | 40 |

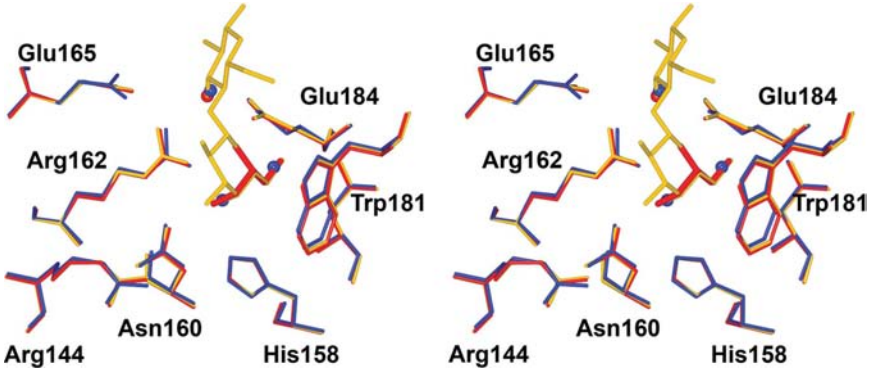


**Figure 3**
The galectin-3 CRD binding site of three superimposed structures showing the relative positions of lactose, glycerol and water molecules. Depicted are the lactose-containing structure (yellow; PDB code 2nn8), the structure containing glycerol (and one water) (red; PDB code 2nmo) and structure containing water only (blue; PDB code 2nmn). Waters are represented as spheres.

of 80–90%, respectively. An X-ray diffraction data set collected at room temperature from a crystal soaked in reservoir solution for 17 d (2.45 Å, Table 1) revealed that some lactose had diffused out of the binding site. The difference electron-density maps contoured at 2.0$\sigma$ provided evidence that lactose still occupied a percentage of binding sites within the crystal and we estimated 40% occupancy. Three water molecules were well defined in the binding site (Fig. 2*b*; PDB code 2nmn) and superimposition of the water-bound structure with the lactose-bound structure showed that these waters occupied the same positions as O4 and O6 of galactose and O3 of glucose in the lactose structure (Fig. 3), highlighting that hydrogen-bond interactions with these groups are important for stabilization of the ligand.

A galectin-3 lactose cocrystal that was soaked in reservoir solution for 29 d, designed to remove lactose, prior to a brief cryosoak [~1 min in reservoir solution supplemented with 15%(*v*/*v*) glycerol] revealed a clearly defined glycerol molecule within the binding site (Fig. 2*c*; PDB code 2nmo; Table 1). Interestingly, the glycerol molecule adopts a conformation identical to the atoms of the galactose residue in the lactose-bound structures. The three C atoms of glycerol occupy the same sites as C4, C5 and C6 of galactose, while the three glycerol O atoms occupy identical sites to O1, O4 and O6 of galactose. A water molecule is also present adjacent to the glycerol at the site equivalent to that occupied by O3 of glucose in the lactose-containing structures (Fig. 3). Lactose is partially present, however, as difference electron-density maps contoured at 2.5$\sigma$ calculated after inclusion of glycerol in the refinement model showed linked density that builds a galactose residue and those at 1.4$\sigma$ also gave indication of the glucose ring. We estimate an occupancy of 30% for the lactose. In crystals where lactose had not previously been allowed to diffuse out, glycerol was unable to displace lactose over the short time frame of the cryosoak (Fig. 2*a*).

In the water-bound and glycerol-bound galectin-3 structures, the amino-acid side chains within the binding site and the loop regions on either side of the binding groove are determined as being identical to those in the lactose-bound structures. This contrasts with the NMR results of the galectin-3 CRD, in which the loops around the binding site undergo a conformational change in the absence of ligand (Umemoto *et al.*, 2003). This discrepancy is a consequence of crystal packing, as intermolecular contacts occur between the loop regions and symmetry-related molecules. A similar finding has been observed with HIV-1 reverse transcriptase, where an open form of the unliganded structure was obtained after soaking out the ligand from pre-formed crystals (Esnouf *et al.*, 1995), while apo crystal forms of the protein were found to adopt a closed conformation (Hsiou *et al.*, 1996; Rodgers *et al.*, 1995). It was subsequently shown that both forms of the protein exist as an equilibrium in solution (Kensch *et al.*, 2000).

Although lactose requires weeks to diffuse from cocrystals, glycerol enters the binding site in seconds to minutes. This was unexpected considering the low affinity of the lactose ligand ($K_d$ = 260 $\mu M$) and the open access to adjacent solvent channels. A major contributor to this variance will be the presence of a large glycerol concentration gradient driving glycerol into the crystal during cryoprotection soaks. Although the affinity of galectin-3 for glycerol is likely to be very low, at this high concentration (2 $M$) the affinity ($K_d$) only needs to be ~200 m$M$ for the occupancy in the binding site to reach 90% (using the fractional saturation equation of Danley, 2006). Additionally, the smaller radius of gyration and greater flexibility of glycerol compared with lactose would be likely to contribute to a higher rate of diffusion though solvent channels (Geremia *et al.*, 2006). Our experimental results of a slow diffusion rate for lactose removal and a fast diffusion rate of glycerol into our galectin-3 CRD crystals correlate with the quantitative computational approach for estimating soaking times of small ligands into and out of protein crystals (Geremia *et al.*, 2006). Using our experimental conditions with this computational approach

indicated that lactose can freely diffuse through the solvent channels and requires approximately 9 d to reduce to less than 20% occupancy. This is a close approximation to our experimental results and offers support for the utilization of these prediction methods in the design of soaking experiments for SADD. Glycerol was unable to displace bound lactose over the short time frame of the cryoprotectant soak, whereas prior soaking out of lactose enabled the generation of a glycerol-bound structure. The prior soaking out of cocrystallized ligands may be of use for ligand exchange in SADD, especially in cases where the affinity of the new ligand of interest is very low or unknown. Additionally, after prior soaking out of a cocrystallized ligand the soaking time of a new ligand into the crystal may be greatly reduced, which would be beneficial in cases where low ligand solubility requires the use of high concentrations of organic solvents or DMSO, which may affect protein crystals during long soaks.

We thank the staff at beamline 8.3.1 at the Advanced Light Source (ALS) for assistance in crystallographic data collection. Beamline 8.3.1 at the Lawrence Berkeley National Laboratory, Advanced Light Source was funded by the NSF, the University of California and Henry Wheeler. Stacy Scott is thanked for assistance in establishing the expression protocols of galectin-3 in-house. We acknowledge financial support from the Access to Major Research Facilities Programme, a component of the International Science Linkages Programme established under the Australian Government's innovation statement Backing Australia's Ability.

## References

Barondes, S. H., Cooper, D. N., Gitt, M. A. & Leffler, H. (1994). *J. Biol. Chem.* **269**, 20807–20810.
Collaborative Computational Project, Number 4 (1994). *Acta Cryst.* D**50**, 760–763.
Danley, D. E. (2006). *Acta Cryst.* D**62**, 569–575.
Emsley, P. & Cowtan, K. (2004). *Acta Cryst.* D**60**, 2126–2132.
Esnouf, R., Ren, J., Ross, C., Jones, Y., Stammers, D. & Stuart, D. (1995). *Nature Struct. Biol.* **2**, 303–308.
Evans, P. R. (1993). *Proceedings of the CCP4 Study Weekend. Data Collection and Processing*, edited by L. Sawyer, N. Isaacs & S. Bailey, pp. 114–122. Warrington: Daresbury Laboratory.
Gallop, P. M., Seifter, S. & Meilman, E. (1957). *J. Biol. Chem.* **227**, 891–906.
Geremia, S., Campagnolo, M., Demitri, N. & Johnson, L. N. (2006). *Structure*, **14**, 393–400.
Hirabayashi, J., Hashidate, T., Arata, Y., Nishi, N., Nakamura, T., Hirashima, M., Urashima, T., Oka, T., Futai, M., Muller, W. E., Yagi, F. & Kasai, K. (2002). *Biochim. Biophys. Acta*, **1572**, 232–254.
Holton, J. & Alber, T. (2004). *Proc. Natl Acad. Sci. USA*, **101**, 1537–1542.
Hsiou, Y., Ding, J., Das, K., Clark, A. D. Jr, Hughes, S. H. & Arnold, E. (1996). *Structure*, **4**, 853–860.
Hughes, R. C. (2001). *Biochimie*, **83**, 667–676.
Jones, T. A., Zou, J.-Y., Cowan, S. W. & Kjeldgaard, M. (1991). *Acta Cryst.* A**47**, 110–119.
Kendrew, J. C. & Moelwyn-Hughes, E. A. (1940). *Proc. R. Soc. London*, **176**, 352–367.
Kensch, O., Restle, T., Wohrl, B. M., Goody, R. S. & Steinhoff, H. J. (2000). *J. Mol. Biol.* **301**, 1029–1039.
Laskowski, R. A., MacArthur, M. W., Moss, D. S. & Thornton, J. M. (1993). *J. Appl. Cryst.* **26**, 283–291.
Leffler, H., Masiarz, F. R. & Barondes, S. H. (1989). *Biochemistry*, **28**, 9222–9229.
Leslie, A. G. W. (2006). *Acta Cryst.* D**62**, 48–57.
Levi, G. & Teichberg, V. I. (1981). *J. Biol. Chem.* **256**, 5735–5740.
McNae, I. W., Kan, D., Kontopidis, G., Patterson, A., Taylor, Paul., Worrall, L. & Walkinshaw, M. D. (2005). *Crystallogr. Rev.* **11**, 61–71.
Massa, S. M., Cooper, D. N., Leffler, H. & Barondes, S. H. (1993). *Biochemistry*, **32**, 260–267.
Murshudov, G. N., Vagin, A. A. & Dodson, E. J. (1997). *Acta Cryst.* D**53**, 240–255.
Ochieng, J., Furtak, V. & Lukyanov, P. (2004). *Glycoconj. J.* **19**, 527–535.
Robertson, M. W., Albrandt, K., Keller, D. & Liu, F. T. (1990). *Biochemistry*, **29**, 8093–8100.
Rodgers, D. W., Gamblin, S. J., Harris, B. A., Ray, S., Culp, J. S., Hellmig, B., Woolf, D. J., Debouck, C. & Harrison, S. C. (1995). *Proc. Natl Acad. Sci. USA*, **92**, 1222–1226.
Saiki, R. K., Scharf, S., Faloona, F., Mullis, K. B., Horn, G. T., Erlich, H. A. & Arnheim, N. (1985). *Science*, **230**, 1350–1354.
Seetharaman, J., Kanigsberg, A., Slaaby, R., Leffler, H., Barondes, S. H. & Rini, J. M. (1998). *J. Biol. Chem.* **273**, 13047–13052.
Sorme, P., Arnoux, P., Kahl-Knutsson, B., Leffler, H., Rini, J. M. & Nilsson, U. J. (2005). *J. Am. Chem. Soc.* **127**, 1737–1743.
Stillman, B. N., Hsu, D. K., Pang, M., Brewer, C. F., Johnson, P., Liu, F. T. & Baum, L. G. (2006). *J. Immunol.* **176**, 778–789.
Takenaka, Y., Fukumori, T., Yoshii, T., Oka, N., Inohara, H., Kim, H. R., Bresalier, R. S. & Raz, A. (2004). *Mol. Cell. Biol.* **24**, 4395–4406.
Umemoto, K., Leffler, H., Venot, A., Valafar, H. & Prestegard, J. H. (2003). *Biochemistry*, **42**, 3688–3695.
Yang, R. Y., Hsu, D. K. & Liu, F. T. (1996). *Proc. Natl Acad. Sci. USA*, **93**, 6737–6742.